

# Noble Metal Doped Optical Fiber for Specialty Light Source

Rik Chattopadhyay, Arindam Haldar, Mukul C. Paul  
and Shyamal K. Bhadra

**Abstract** We report noble metal doped optical fiber which is suitable for laser and helps enhancing fluorescence when it is doped with active elements. Silver nano-clusters (average diameter 1.5 nm) in the core of a standard step index fiber are doped using standard fiber fabrication method. These fibers show broad visible fluorescence in the wavelength range 420–700 nm under 405 nm excitation. This appears to occur due to long interaction length of pump light with the metal nano-clusters and quantum confinement effect. We observe enhanced fluorescence from rare earth ions (i.e.  $\text{Tm}^{3+}$  and  $\text{Yb}^{3+}$ ) in presence of silver nano-clusters when the optimized length of the fiber is pumped by using 980 nm fiber-pig-tailed laser diode. The experimental results are explained with the help of analytical and quantum mechanical models. These fibers would be helpful to make efficient optical fiber based light sources mostly in the visible range.

## 1 Introduction

Conventional fiber based light source is made with the help of rare earth (RE) doped optical fiber where the core glass is doped with RE ions such as  $\text{Tm}^{3+}$ ,  $\text{Yb}^{3+}$ ,  $\text{Er}^{3+}$  etc. with limited fluorescence emission efficiency. The absorption and emission cross-sections of the RE ions in silica glass are insufficient to produce large optical emission band with available commercial pumping sources. Since

---

R. Chattopadhyay · A. Haldar · M.C. Paul · S.K. Bhadra  
Fiber Optics and Photonics Division, CSIR-Central Glass and Ceramic Research Institute,  
196 Raja S. C. Mullick Road, Kolkata 700032, India

A. Haldar  
Optoelectronics Research Centre, University of Southampton, B53,  
Southampton, SO17 1BJ, UK

R. Chattopadhyay · S.K. Bhadra (✉)  
Raman Centre for Atomic, Molecular and Optical Sciences, Indian Association  
for the Cultivation of Science (IACS), Kolkata 700032, India  
e-mail: rcskb@iacs.res.in

noble metal-nano-clusters (MNCs) have interesting optical properties when they are doped in dielectric materials, we tried to dope some noble metals, especially Silver (Ag) nanoclusters (NCs) in the fiber core to fabricate a new family of fluorescent fiber which are capable of producing fluorescence emission without RE ions. On the other hand the characteristics fluorescence emission of RE doped fiber is enhanced in presence of MNCs. The main challenge in synthesis of MNCs in dielectric host is to maintain the desired structural stability. Without any scaffold the clusters tend to aggregate to larger particle, which is an irreversible process as it happens in fluid. It would be an added advantage if these Ag-NCs are synthesized in the core glass of an optical fiber to get niche properties. The immobility of the clusters will prevent aggregation of the NCs. Furthermore enhanced fluorescent output could be possible in the visible regime due to the long interaction length of propagating optical field with MNCs in fiber core. In order to understand the intricacies of the process we resort to some standard theoretical and numerical models that explain the experimental results quite satisfactorily.

## 2 Fluorescence from Ag NCs

The optical properties of MNCs differ considerably from those of the bulk metals due to confinement of conduction electrons [1]. The optical properties of particles with diameter ( $>10$  nm) can be explained using classical Mie theory [2] or some finite element methods [3]. As the particle size reduces, the number of surface atoms increases dramatically, implying a change of the physical environment of the NCs [4]. In addition, systems with countable number of atoms, electrons are confined and the electronic densities of states become discrete, which bring discrete features to the dielectric spectra, namely, the quantum size effect. Both effects drive the dielectric characteristics of NCs to deviate from the bulk. The classical Drude model incorporates the surface effect on the conduction electrons. In case of MNCs we also have to consider the effect of bound electrons. The Lorentz model is widely used for this purpose. According to this model the dielectric function is given by:

$$\varepsilon(\omega) = 1 + \frac{\omega_p^2}{\omega_0^2 - \omega^2 - i\gamma\omega} \quad (1)$$

where  $\omega_p$  is the plasmon resonance frequency,  $\omega_0$  is the Lorentz frequency,  $\gamma$  is the damping factor and  $\omega$  is the frequency of incident light. In general the Lorentz parameters are constant for bulk metals but in case of MNCs the Density Functional Theory (DFT) shows that there exists certain frequency below which the intraband transition of electrons takes place and the property of the MNC can be approximated by the Lorentz model [5]. Hence the Lorentz parameters became a function

**Table 1** Parameters used in (2)

Parameters	$a_1$	$a_2$	$a_3$	$b_1$	$b_2$
Values	$1.95 \text{ nm}^{-1}$	$0.18 \text{ eV}^{-1}$	$0.192 \text{ nm eV}$	$0.198 \text{ nm}^{-1} \text{ eV}^{-1}$	$0.62 \text{ nm}$

of the NC radius and the imaginary part of the dielectric function can be written as He and Zeng [5]:

$$\varepsilon_{Imag}(\omega r) = \frac{\omega_p^2 \left[1 - e^{(a_1 r)^2}\right]^2 \left(\gamma + \frac{a_3}{\hbar r}\right) \left[1 - e^{(r^3/b_2^3)}\right] \omega}{\left[\frac{1}{\hbar^2} \left(\frac{1}{a_2 + b_1 r}\right)^2 - \omega^2\right]^2 + \left[\left(\gamma + \frac{a_3}{r}\right) \left(1 - e^{(r^3/b_2^3)}\right) \omega\right]^2} \quad (2)$$

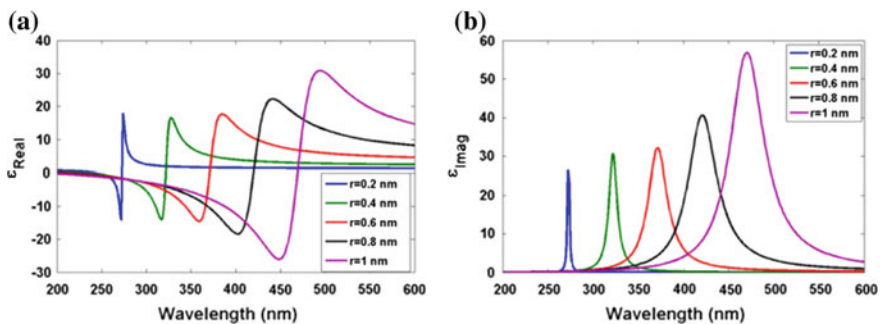
The parameters  $a$ 's and  $b$ 's are given in Table 1. We have used  $\hbar\omega_{p,bulk} = 7.24 \text{ eV}$  and  $\hbar\gamma_{bulk} = 0.0685 \text{ eV}$  [5].

After getting the imaginary part we can readily derive the real part of the permittivity using the Kramer-Kronig relation given by:

$$\varepsilon_{Real}(\omega r) = 1 + \frac{2}{\pi} P \int_0^{\infty} \frac{\varepsilon_{Imag}(r, \omega') \omega'}{\omega'^2 - \omega^2} d\omega' \quad (3)$$

where 'P' denotes principal value integral. Using (2) and (3) we can calculate the dielectric permittivity of MNCs. Figure 1 shows the dielectric permittivity of MNCs with different radius in vacuum.

When these MNCs are doped in a dielectric material, the effective permittivity of the composite material can be estimated by using Maxwell Garnett effective medium theory owing to the approximation that the MNCs are not connected to each other. In this case the effective permittivity is given by Koledintseva et al. [6]:

**Fig. 1** Variation of dielectric permittivity (real and imaginary) with particle radius

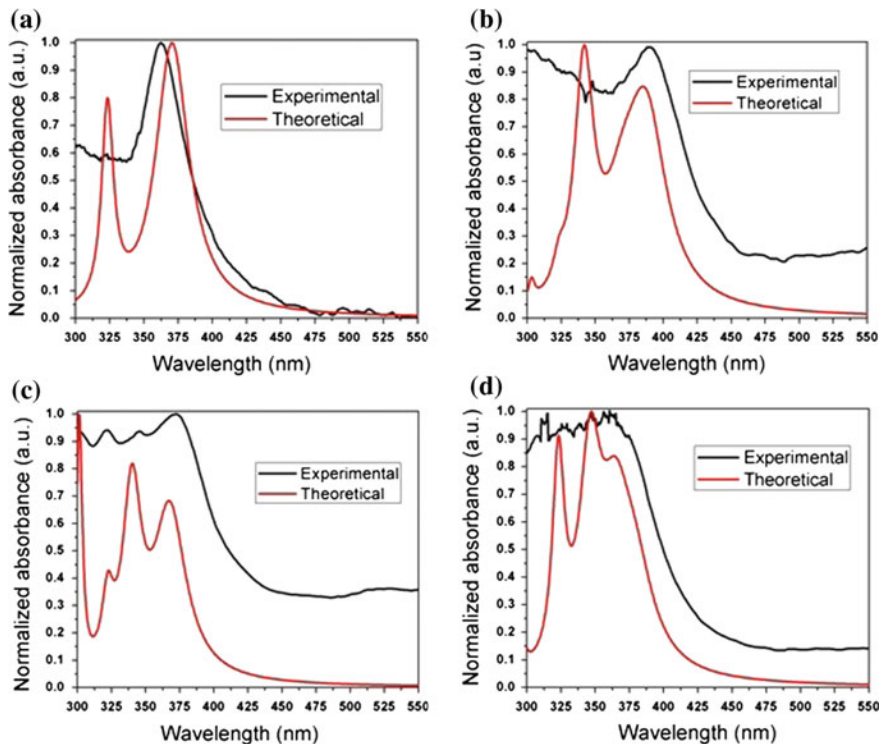


**Fig. 2** Theoretical and experimental absorption spectra of fiber samples **a** AMNC-1, **b** AMNC-2, **c** AMNC-3 and **d** AMNC-4

$$\epsilon_{eff} = \epsilon_{host} + \frac{\sum_{i=1}^n f_i (\epsilon_{i,metal} - \epsilon_{host}) \frac{3\epsilon_{host}}{\epsilon_{i,metal} + 3\epsilon_{host}}}{1 - \sum_{i=1}^n f_i \frac{\epsilon_{i,metal} - \epsilon_{host}}{\epsilon_{i,metal} + 2\epsilon_{host}}} \quad (4)$$

where  $f_i$  denotes volume fraction of  $i$ -th MNC in host. With the help of (2) and (3) we can calculate the permittivity of each type of MNC. Then using (4) we determine the effective permittivity and absorption coefficient of the core glass of the fabricated MNC doped fibers and verified them with the experimentally measured absorption spectrum of different samples. The results are shown in Fig. 2. The experimental and theoretical results are in good agreement. The finite size of the MNCs makes the electronic energy bands discrete. Hence we may assume that electrons will undergo band transition when excited by proper excitation energy. Therefore such MNCs in glass matrix can show fluorescence if we excite the composite glass sample with light with appropriate frequency. The electronic structure of these few atom clusters can be explained with the help of spherical jellium model. Though this model is proposed for alkali metals but it works

satisfactorily in case of noble metals also, as they have single electron in the outer most orbit. According to this model the electrons in a MNC is distributed in different energy shells of a spherical harmonic potential well. Later Clemenger showed that for clusters having atoms  $\geq 20$  the potential is anharmonic and is given by Diez et al. [7]:

$$H = -\frac{p^2}{2m} + \frac{m\omega_0^2 q^2}{2} - U\hbar\omega_\Delta \left( l^2 - n \frac{(n+3)}{6} \right) \quad (5)$$

where  $p$  and  $q$  are the momentum and position operators of the single-electron respectively,  $l$  is the angular momentum,  $n$  is the shell number and  $U$  is the anharmonic distortion parameter which depends on the size of the cluster. The transition energy of the electrons can be written as Diez et al. [7]:

$$\Delta E = \frac{E_F r_s}{R} \left[ 1 - U \left( l_e^2 - l_g^2 - \frac{n+2}{3} \right) \right] \quad (6)$$

where  $l_e$  and  $l_g$  represent the angular momentum of excited and ground states respectively. The values taken for Ag are  $r_s = 3.02$  atomic unit,  $E_F = 5.49$  eV. It is to be noted that there is no direct measurement technique of  $U$ . We choose the value by comparing the theoretical results with experimental observation. The experimentally measured emission spectrum and theoretically calculated transition probability for different emission lines of Ag NCs in our fabricated sample shows good agreement. The results are given in [8]. We observed that all calculated emission lines fall within the measured fluorescence band. This confirms the presence of Ag NCs in the fiber core glass and indicates that such fluorescence occur due to electronic band transition. We excited our fiber samples with a 405 nm pig-tailed laser diode of output power 50 mW.

### 3 Fluorescence Enhancement of RE by MNC

We have observed the fluorescence from Ag NCs doped optical fiber due to discontinuity in the energy bands. These discrete energy bands of the NCs serves another purpose in fluorescence light emission. We observed that when such clusters are codoped with conventional RE ions in the fiber core, the fluorescence emission from the RE increases in presence of MNCs. For large size MNPs such phenomena were observed and attributed as metal enhanced fluorescence (MEF) [9]. MEF explains the enhancement in fluorescence radiation with the help of radiative decay engineering. This theory states that larger MNPs produces localized electromagnetic (EM) field as they act as an dipole antenna. We calculated the local field enhancement factor for the Ag NCs present in our fabricated fiber samples. Since we codoped Ag NCs with  $\text{Yb}^{3+}$  and  $\text{Tm}^{3+}$  and excited the system

with 975 nm laser diode to get resonant energy transfer (ET) between  $\text{Yb}^{3+}$  and  $\text{Tm}^{3+}$ , so we have to calculate the local field at 975 nm.

The calculated value comes out close to 1 indicating that MEF should not take place for such small NCs. It may happen that the MNCs may alter the ET process between  $\text{Yb}^{3+}$  and  $\text{Tm}^{3+}$ . So we measured the fluorescence energy at each emission line of the RE present in the system. The log-log plot of  $\text{Yb}^{3+}$  emission energy with that of  $\text{Tm}^{3+}$  is linear and the slope of the graphs represents number of photons involved in the ET process. We generated the graphs for our fabricated samples and found out that MNCs does not affect the ET process. Yet we observed an enhancement in the fluorescence of all the RE present in the system due to MNC, which is unconventional because in resonance ET process emission from one RE ion increases at the expense of other. Simultaneous enhancement was not observed. The fluorescence lifetime of the RE decreases in the presence of MNC. This property appears to be unusual. The results are shown in Fig. 3 [10]. Since MEF is inadequate to explain this enhancement mechanism therefore we apprehend the radiation coupling between MNC and RE is different. In next step we try to explain the presence of both MNCs and fluorophores together as a coupled system accordingly we have evaluated the dynamics of the coupled system from a quantum mechanical point of view. Subsequent studies show that this typical nature where MNCs act as an oscillating dipole in IR region is misleading. The MNC might be visualized as a single dipole if the electrons present in the system execute coherent oscillation. That may not be valid for such ultra-small metal particles.

We have already seen that the energy band of the electrons in MNC becomes discrete. These clusters behave as insulating cluster as the Kubo gap which is

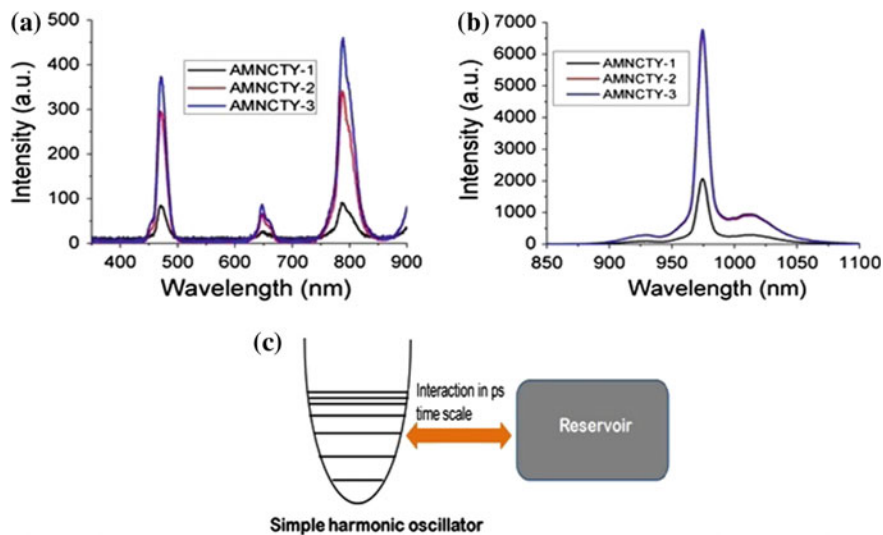


**Fig. 3** Emission spectra of AMNCTY fibers **a** 350–850 nm and **b** 900–1100 nm. AMNCTY-1 sample does not contain Ag NCs [10] **c** the schematic of interaction between MNC and rare earth ion

greater than  $k_B T$  [11]. In the present case the electrons in MNC have closely spaced density of states (Kubo states) [11] with energy gap  $\delta = 4E_F/3N$ , where  $E_F$  is the Fermi energy and  $N$  is the number of valence electron of the MNC. The most probable cluster radius ( $\sim 0.65$  nm) as obtained from TEM analysis has  $\delta \sim 0.13$  eV. The pump wavelength (975 nm) provides energy greater than this but less than that required for radiative transition [12]. Hence radiative transition of electrons is not possible. But electron can non-radiatively decay among various energy bands available in the valence band. So we may consider the MNC to be acting as a reservoir of many electronic oscillators having random frequencies and damping constant. From quantum mechanical point of view the rare earth ion can be visualized as a simple harmonic oscillator (SHO). The average damping time of electrons in Ag NCs is  $\sim 16.6$  fs [3] on the other hand the radiative decay time of  $\text{Yb}^{3+}$  form  $^2F_{5/2}$  state is  $\sim 924$   $\mu\text{s}$ . Therefore in the interaction picture of MNC and  $\text{Yb}^{3+}/\text{Tm}^{3+}$  we may consider that the rare earth stays in its corresponding excited state while interacting with the MNC. So in our model we assumed that the simple harmonic oscillator does not lose photon while the reservoir loses photon at some rate,  $\gamma$ . The schematic of the interaction picture is given in Fig. 3c.

The interaction of the system can be represented by a system Hamiltonian, where we consider the interaction is instantaneous and takes place at a resonant frequency. In our case the frequency corresponds to the pump signal at 975 nm. The evolution of the system is then represented by density matrix and the solution indicates that both the RE oscillation and the electron oscillation in MNC will decay at rate slower than the rate at which oscillation in the reservoir dies. Since MNCs act as reservoir and the oscillation in MNCs dies at within few fs, hence the RE oscillation will die faster than in the absence of MNC. This explains the lifetime decrease in presence of MNC.

This model explains the reduction in fluorescence lifetime of the  $\text{Yb}^{3+}$  and  $\text{Tm}^{3+}$  in presence of Ag NCs. Still, we observe enhanced fluorescence. This can be explained from the ground state absorbance of the AMNCTY samples. We observed that the absorption cross-section of all the rare earth increases in presence of Ag NCs. This enhanced absorption cross-section can be explained from this coupled model. Here we consider the MNC as a receiver and the rare earth ion acts as an antenna. The incident light is now strongly scattered by the rare earth ion and leads to an enhanced intensity in the position of Ag NC. Therefore larger dissipation of energy in MNC occurs. This does not lead to quantum quenching because the change in radiative and non-radiative decay rate of the molecule is very small as the distance between Ag NC and RE element is greater than the size of NCs [13]. This leads to enhanced absorption of the  $\text{Yb}^{3+}$  in presence of Ag NCs under coherent excitation and we observed enhanced fluorescence. Therefore we observed simultaneous fluorescence enhancement of  $\text{Tm}^{3+}$  and  $\text{Yb}^{3+}$  when Ag NCs are present in the system.

## 4 Fabrication and Material Analysis of Fabricated Core Glass of Ag-NCs and Ag-NCs Along with RE Doped Optical Fibers

Ag-NCs as well as Ag-NCs along with  $Tm^{3+}$  and  $Yb^{3+}$  doped aluminosilica glass optical preforms were fabricated using modified chemical vapour deposition process along with solution doping technique (MCVD-SD) [8, 10]. Different solutions were used having different concentration of the  $AgNO_3$ ,  $Tm(NO_3)_3$  and  $Yb(NO_3)_3$  maintaining a constant concentration of  $Al(NO_3)_3$  to create varying dopant concentration in the fabricated fibers. The compositions of the different fabricated preform core glasses are given in Table 2. Using these preforms, optical fibers of 125  $\mu m$  diameter were fabricated using silica fiber draw tower at a drawing temp of 2050  $^{\circ}C$ . The MCVD set up and some fabricated Ag doped preform are shown in Fig. 4a, b. The refractive index profiles (RIP) of fabricated preforms were measured by optical perform analyser (PK 2600). From the RIPs, the numerical apertures of the fibers were calculated for 630 nm wavelength (Table 2).

To confirm the presence of Ag in the fiber core we have performed energy dispersive X-ray spectroscopy (EDS) of the fiber sample along its cross-sectional diameter. The result for AMNC-1 sample is shown in Fig. 4c. It reveals the presence of metallic Ag in the core glass. The core glass microstructures were analyzed by the transmission electron microscope (TEM), using thin film sampling technique (Fig. 5a–c). The images clearly show the presence of nano-particles into the core glass. The spot EDX analysis was also performed to get the structural information of the particles into the core glass (Fig. 5d). The electron diffraction (ED) was also performed to investigate the nature of the dopants into the core i.e. either amorphous or crystalline (Fig. 5d).

The XPS analysis was also performed using the same thin film sample to identify the exact oxidation state of Ag into the core glass (Fig. 5e). The peaks appeared in the XPS spectra confirms that the clusters present in the fiber are pure metallic clusters. These analyses show that Metallic Ag NCs are present in the core glass of

**Table 2** Composition details of synthesis fibers

Sample id	Solution used	NA
AMNC-1	1.5(M) $AgNO_3$ – 1.0(M) $Al(NO_3)_3$	0.19
AMNC-2	1.75(M) $AgNO_3$ – 1.0(M) $Al(NO_3)_3$	0.15
AMNC-3	1.5(M) $AgNO_3$ – 1.0(M) $Al(NO_3)_3$	0.16
AMNC-4	1.0(M) $AgNO_3$ – 1.0(M) $Al(NO_3)_3$	0.17
AMNCTY-1	0.02(M) $Tm(NO_3)_3$ – 0.03(M) $Yb(NO_3)_3$ – 1.0(M) $Al(NO_3)_3$ – 0.0(M) $AgNO_3$	0.13
AMNCTY-2	0.02(M) $Tm(NO_3)_3$ – 0.03(M) $Yb(NO_3)_3$ – 1.0(M) $Al(NO_3)_3$ – 1.75(M) $AgNO_3$	0.15
AMNCTY-3	0.02(M) $Tm(NO_3)_3$ – 0.03(M) $Yb(NO_3)_3$ – 1.0(M) $Al(NO_3)_3$ – 1.5(M) $AgNO_3$	0.17



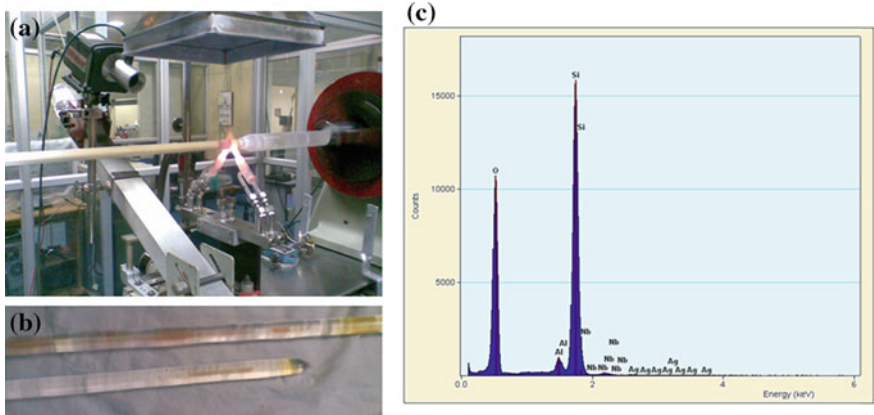


**Fig. 4** a Sintering process during AMNC-2 preform fabrication showing yellow coloration at the tube wall and b Ag-NCs doped optical preforms. c EDS of AMNC-1 fiber along cross-sectional diameter

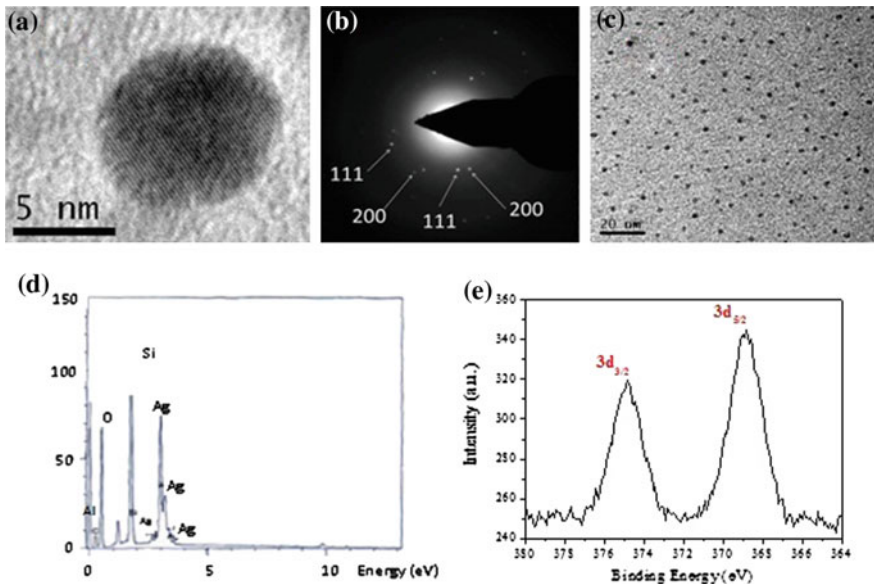


**Fig. 5** a HR-TEM image of a large Ag particle obtained in one of the fabricated fiber sample b electron diffraction pattern along with crystallographic planes taken on the Ag particles of (a), c TEM image of Ag MNC doped fiber core glass, and d spot EDX spectra taken on the Ag particles at the core of Ag doped fiber [8], e XPS spectra of Ag particle of Ag MNC doped fiber, show two peaks at 374.8 and 368.8 eV for spin-orbit split peaks of Ag 3d<sub>3/2</sub> and 3d<sub>5/2</sub> representing the ‘zero’ oxidation state of Ag

our fabricated fibers. The electron diffraction analysis also helps us to generate an idea about the structural geometry which is needed while calculating shell number in jellium model. The TEM analysis helps us to create the NCs size distribution data in the fabricated samples. These information is vital for implementation of (4). Using these characterization technique along with our theoretical model we explain the unique fluorescence of the Ag NC doped fiber samples. The results are in good agreement indicating that their uniqueness originates from the MNCs.

## 5 Conclusions

In conclusion we claim that Ag MNC doped optical fiber possesses unique fluorescence property. When excited by adequate energy the MNC itself shows fluorescence. On the other hand if these fibers are codoped with RE ions and suitably pumped they show enhanced fluorescence of the RE ions without altering the ET process between the RE ions. These fibers can form a new family of fibers based low threshold light sources.

**Acknowledgements** Part of the work of RC & SKB is supported by CSIR Emeritus Scientist Scheme-21(1017)/15/EMR-II. Authors are indebted to Director, CSIR-CGRI, Kolkata for his support and encouragement and Director, IACS, Kolkata for his unstinted cooperation.

## References

1. Scholl J. A., Koh A. L. and Dionne J. A., Quantum plasmon resonances of individual metallic nanoparticles, *Nature*, 483, 421–427 (2012).
2. Mie G., contributions to the optics of turbid media, particularly solution of colloidal metals, *Ann. der Physik.*, 25, 377–445 (1908).
3. Kelly K. L. et. al., The Optical Properties of Metal Nanoparticles: The Influence of Size, Shape, and Dielectric Environment, *J. Phys. Chem. B*, 107, 668–677 (2003).
4. Baletto F. and Ferrando R., Structural properties of nanoclusters: Energetic, thermodynamic, and kinetic effects, *Rev. Mod. Phys.*, 77, 371–423 (2005).
5. He Y. and Zeng T., First-Principles Study and Model of Dielectric Functions of Silver Nanoparticles, *J. Phys. Chem. C*, 114, 18023–18030 (2010).
6. Koledintseva M. Y. et. al., Representation of permittivity for multi-phase dielectric mixtures in FDTD modeling, *International Symposium on Electromagnetic Compatibility (EMC 2004) IEEE.*, 1, 309–314 (2004).
7. Diez I. et. al., Blue, green and red emissive silver nanoclusters formed in organic solvents, *Angew. Chem. Int. Ed.*, 48, 2122–2125 (2009).
8. Halder A. et. al., Highly fluorescent silver nanoclusters in alumina-silica composite optical fiber, *Appl. Phys. Lett.*, 106, 2, 011101 (2015).
9. Guzатов D. V., Plasmonic enhancement of molecular fluorescence near silver nanoparticles: Theory, modeling, and experiment, *J. Phys. Chem. C*, 116, 10723–10733 (2012).
10. Chattopadhyay R. et. al., Quantum sized Ag nanocluster assisted fluorescence enhancement in  $\text{Tm}^{3+}$ - $\text{Yb}^{3+}$  doped optical fiber beyond plasmonics *Appl. Phys. Lett.*, 107, 233107 (2015).

11. Morton S. M., Silverstein D. W., and Jensen L., Theoretical studies of plasmonics using electronic structure methods, *Chem. Rev.*, 111, 3962–3994 (2011).
12. Maurizio C. et. al., Enhancement of the  $\text{Er}^{3+}$  luminescence in Er-doped silica by few-atom metal aggregates, *Phys. Rev. B*, 83, 195430 (2011).
13. Pandozii F. et. al., A spectroscopic analysis of blue and ultraviolet upconverted emissions from  $\text{Gd}_3\text{Ga}_5\text{O}_{12}:\text{Tm}^{3+}$ ,  $\text{Yb}^{3+}$  nanocrystals, *J. Phys. Chem. B*, 109, 17400–17405 (2005).